THE JOURNAL OF PHYSICAL CHEMISTRY C

Article

pubs.acs.org/JPCC

Instability of Poly(ethylene oxide) upon Oxidation in Lithium−Air Batteries

Jonathon R. Harding,[†] Chibueze V. Amanchukwu,[†] Paula T. Hammond,[†] and Yang Shao-Horn*[,‡,§]

[†]Department of Chemical Engineering, [‡]Department of Mechanical Engineering, and [§]Department of Materials Science & Engineering, Massachusetts Institute of Technology, 77 Massachusetts Ave., Cambridge, Massachusetts 02139, United States

Supporting Information

ABSTRACT: The instability of aprotic and polymer electrolytes in Li−air batteries limits the development of these batteries for practical use. Here, we investigate the stability of an electrolyte based on poly(ethylene oxide) (PEO), which has been used extensively for polymer Li-ion batteries, during discharge and charge of Li−O_2 batteries. We show that applying potentials greater than open circuit voltage (OCV, ~3 V_{Li}), which is typically required for Li−O_2 battery charging, increases the rate of PEO auto-oxidation in an oxygenated environment, with and without prior discharge. Analysis on the rate of reaction, extent of oxidation, and the oxidation products allows us to propose that rate of spontaneous radical formation in PEO is accelerated at applied potentials greater than OCV. We also suggest that the phenomena described here will still occur in ether-based electrolytes at room temperature, albeit at a slower rate, and that this will prevent the use of such electrolytes for practical long-lived Li−air batteries. Therefore, PEO-based electrolytes are unsuitable for use in Li−air batteries.

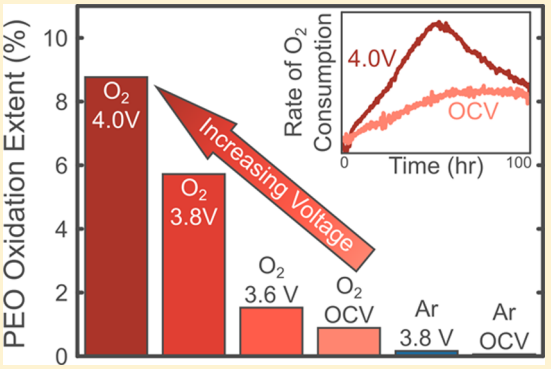

INTRODUCTION

The development and commercialization of lithium-ion batteries over the past 35 years have enabled the recent proliferation of lightweight and long-lived electronic devices such as smartphones and laptops and of electric vehicles with extended ranges.[1,2] However, current lithium-ion materials are nearing their practical limit of specific energy and energy density.[1−3] To develop the next generation of batteries, attention has turned to conversion-type lithium batteries,[1] such as lithium−sulfur and lithium−air (Li−air), which rely on the bulk chemical conversion of materials within the electrodes during discharge and charge. In particular, Li−air batteries have been investigated as a promising avenue for this next generation of batteries, as their theoretical specific energy is 2000 W·h/kg at the cell level,[4] and practical energy density of Li−air batteries is expected to be 150−200% greater than that of practical Li-ion batteries.[5]

In spite of the theoretical promise of Li−air batteries, many challenges must be resolved before practical devices can be produced, including low cycle life, high charging overpotential, and instability of lithium metal at the negative electrode.[4,6] In particular, electrolyte stability has proven to be a significant problem in the operation of Li−air batteries over multiple cycles, and many recent papers have focused on the search for suitable electrolyte solvents that are stable against the lithium peroxide and superoxide species that are produced during discharge.[6−16] Ether-based small molecules and oligomers, such as 1,2-dimethoxyethane (DME) or tetraglyme, have been shown to be moderately stable[8,11,16−18] and have been demonstrated in sealed oxygen cells cycled several times at ambient conditions.[17] Other liquid electrolytes have also been recently investigated for use in Li−air batteries, including *N*,*N*-dimethylformamide,[19] *N*,*N*-dimethylacetamide,[13] and dimethyl sulfoxide,[20,21] which has been observed to react over time with lithium peroxide produced during discharge to form lithium hydroxide.[21]

Although liquid electrolytes have been the primary focus of most Li−air battery research to date, solid electrolytes offer several advantages to practical Li−air batteries, including protection of the lithium anode, prevention of electrolyte loss to the environment, and facilitation of oxygen transport to the reaction surface. Two major categories of solid electrolyte are available for Li−air cells: solid polymer electrolytes and solid ceramic electrolytes, which are varied and based on many different chemical and structural compositions.[22] Lithium conducting ceramic electrolytes have been investigated for use both as an electrolyte membrane (in aqueous and nonaqueous systems)[23−26] and as the catholyte in the air electrode where the Li−O_2 reaction occurs.[27] However, their high density (relative to liquid and polymer electrolytes) and difficult handling requirements motivate research into solid polymer electrolytes, which have densities approaching that of

Received: November 25, 2014
Revised: March 6, 2015
Published: March 10, 2015

DOI: 10.1021/jp511794g
J. Phys. Chem. C 2015, 119, 6947−6955

liquid electrolytes and can be easily processed using low-temperature melt or solvent techniques. Gel polymer electrolytes have been used for Li−air batteries previously,[28] including the first demonstration of a nonaqueous Li−air battery by Abraham.[29] However, recent results by our group have shown that many polymers used in gel polymer electrolytes for lithium-ion batteries are unstable when exposed to lithium peroxide,[30] making them unsuitable for Li−air batteries.

Poly(ethylene oxide) (PEO) has been known as a solid state lithium conductor for more than 30 years,[31] and research during that time has aimed to increase the conductivity, reduce the operating temperature, and improve the mechanical stability of these electrolytes.[32−34] These PEO electrolytes have been shown to have a large electrochemical stability window, forming a stable SEI against lithium metal, and no significant decomposition current below 4.9 V vs lithium (V_{Li}).[35] Furthermore, PEO has been shown to have good conductivity above its melting point (10^{-3} S/cm at 60 °C),[22] and various additives have been used to produce functional lithium-ion batteries using a solid PEO electrolyte.[35] Recently, PEO has been investigated as a solid polymer electrolyte for use in Li−air batteries,[36,37] showing that PEO is more stable than carbonate electrolytes for Li−air batteries[36] and demonstrating a PEO-based Li−air cell that was cycled many times under limited capacity conditions.[37]

In this article, we show that PEO electrolytes that are otherwise suitable for use in Li−air batteries undergo significant oxidation when exposed to oxygen and the potentials needed to charge Li−air batteries. The degradation of PEO is observed to occur regardless of the presence of a carbon-based air electrode or Li−air discharge products. The reaction is observed to proceed more rapidly with increasing potential, resulting in significant liquefaction of the solid polymer electrolyte after less than 100 h at 60 °C. We use NMR to identify the PEO decomposition products as those associated with PEO oxidation. Finally, we propose that the rate of spontaneous formation of radical species in PEO is accelerated with increasing potential and conclude that PEO and PEO-derived polymers are unsuitable for elevated temperature work in Li−air batteries. These results may also have further implications about the long-term stability of ether-based small molecule liquid electrolytes (e.g., DME) at room temperature for Li−air applications.

EXPERIMENTAL METHODS

Poly(ethylene oxide) (PEO, MW ~ 4×10^6 g/mol, <1000 ppm BHT) was obtained from Sigma-Aldrich (USA). Butylated hydroxytoluene (BHT) in PEO can minimize oxidation during normal handling of PEO. For electrochemical applications it has been shown that an antioxidant in the electrolyte will interfere with the electrochemical behavior of the cell,[38] and most battery electrolytes are used without these antioxidants. For most experiments presented here, the BHT in the PEO as supplied by the manufacturer was removed from the PEO via Soxhlet extraction in hexanes under flowing argon gas for at least 24 h. Extracted PEO was dried under vacuum at 50 °C for 48 h before being stored in an argon glovebox (<3 ppm of O_2, <0.1 ppm of H_2O) until needed. Lithium bis-(trifluoromethane)sulfonimide (LiTFSI, 99.95% trace metals basis) was obtained from Sigma-Aldrich (USA) and dried under vacuum at 100 °C for at least 24 h before being transferred to an argon glovebox for storage. Separator material was Celgard C480 (Celgard, USA).

The PEO electrolyte was prepared by mixing PEO and LiTFSI (20:1 mol Li/mol EO) with a mortar and pestle inside an argon glovebox. The electrolyte was mixed until the LiTFSI dissolved in the PEO, resulting in a stiff, white mass. This mixture was then annealed under vacuum at 100 °C for at least 24 h, after which the mixture became clear. The mixture was placed between fluorinated ethylene propylene (FEP) sheets and heat-sealed in a water vapor and oxygen transport resistant bag (Sigma-Aldrich, USA; meets MIL-PRF-131K). This bag was then pressed in a benchtop hot press at 100 °C with a maximum applied load of 1 t per 2 g of electrolyte, slowly increasing pressure to minimize the formation of wrinkles. Shims were used to ensure that the electrolyte film thickness was approximately 150 μm. To include a Celgard interlayer, the electrolyte was cut in half, and each half was pressed separately. These were returned to the glovebox and stacked with a sheet of Celgard C480 in between the two halves of electrolyte. This sandwich was resealed and pressed at 100 °C, with a maximum applied load of 5 t per 2 g of electrolyte. Heat was removed, and the press was allowed to cool to room temperature overnight under load. This allowed the PEO electrolyte to fully impregnate the Celgard film, resulting in a translucent film (if the PEO does not fill the Celgard, the film remains white and exhibits poor ionic conductivity). Once pressed, the electrolyte was returned to a water-free glovebox (<0.1 ppm of H_2O), removed from the bags, and punched into 18 mm diameter disks. The FEP film was left on to prevent electrolyte disks from sticking to each other. These disks were collected in a scintillation vial and stored in an argon glovebox until used.

Vulcan carbon (VC) air electrodes were prepared by mixing VC (Premetek, USA), PEO, and LiTFSI (70% w/w VC, 10:1 mol EO/mol Li) in a planetary ball mill (Fritsch Pulviersette 6, Germany) jar, along with 5 mm diameter zirconia beads. A 50% v/v mixture of ethanol in deionized water were added to the jar before sealing and milling for at least 4 h at 500 rpm. The resulting slurry was deposited onto aluminum foil using a Meyer rod with a wet film thickness of 125 μm. The solvent was allowed to evaporate in air before 0.5 in. diameter disks were punched. These disks were collected in a scintillation vial and dried for at least 24 h at 100 °C under vacuum, before being directly transferred into an argon glovebox and stored until ready for use. The resulting electrodes had an approximate areal carbon density of 0.43 mg VC/cm^2 and a total carbon loading of approximately 0.54 mg in each electrode.

Electrochemical cells were prepared in two different configurations, with and without a porous VC positive electrode, inside an argon glovebox. Cells with a VC electrode were prepared by placing the VC electrode carbon-side down onto the PEO electrolyte, inside the protective FEP sheets. A PTFE rod was used to press the carbon into the electrolyte. The FEP was removed, and the aluminum foil was carefully peeled back, leaving the VC electrode attached to the electrolyte. The mass of the VC electrode was determined by differencing the weight of the electrode/aluminum foil before and after attaching the carbon. Cells without a VC electrode omitted this step. For both types of cell, the other protective FEP sheet was removed from an electrolyte disk and gently pressed into the exposed electrolyte onto a disk of lithium (Chemetall, Germany, 15 mm diameter). Using plastic (nonconductive) tweezers, the second sheet of FEP was removed, and a 316 stainless steel mesh disk (15 mm diameter, 400 mesh) was pressed on top of the VC electrode (if present) or directly onto the electrolyte (for VC-free cells). The

DOI: 10.1021/jp511794g
J. Phys. Chem. C 2015, 119, 6947−6955

completed stack was then placed into the body of a lithium−oxygen cell (designed and produced in our lab, as published previously),[39] a lightweight spring (Lee Spring, USA) was added to provide contact with the cell body, and the cell valves were closed to seal it (see Figure 1). The sealed cell was

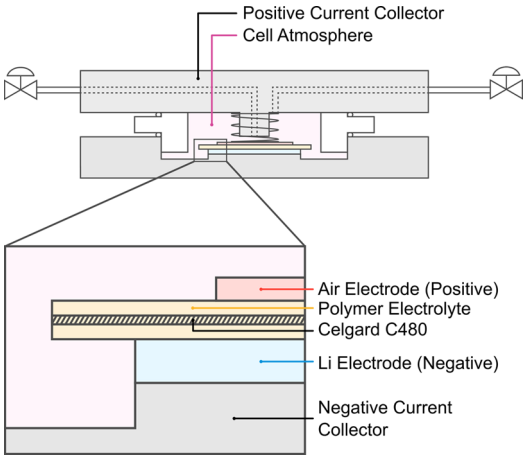

Figure 1. Schematic of the cell used for all tests. Inset shows the structure of the cell and polymer electrolyte, with a Celgard layer inside the polymer electrolyte. The air electrode is either an SS mesh for VC-free cells or a VC electrode.

transferred to a water-free glovebox and purged with oxygen or argon as appropriate. The gas was allowed to flow through the cell at high rate for several seconds to ensure that all the gas in the cell was replaced. The cell was then pressurized to 28 psig (2.9 atm absolute) and sealed, before being removed from the glovebox.

All electrochemical tests were performed at 60 °C, using an ESPEC SU-221 benchtop temperature chamber (ESPEC North America, Inc., USA) and either a Bio-Logic VMP3 multichannel potentiostat (Bio-Logic SAS, France) or a Solartron 1470A multichannel potentiostat (Solartron Analytical, USA). Cells were placed into the heating chamber and immediately connected to a potentiostat for testing. To establish the behavior of PEO electrolytes (without BHT) without applied potential, two cells without VC air electrodes (VC-free cells) were prepared and allowed to rest with an open circuit at 60 °C for 100 h: one in an oxygenated environment and another in an argon atmosphere. Cells that were tested potentiostatically or galvanostatically were rested with an open circuit for 6 h before further testing. At the end of the test, the cells were removed from the heating chamber and transferred into a dry glovebox, where the oxygen from the cell was purged out, before being disassembled, and the PEO electrolyte was stored in an argon glovebox.

Pressure tracking experiments were performed by connecting a cell to a custom-built apparatus based on the design published by McCloskey et al. for a differential electrochemical mass spectrometer (DEMS).[10] Mass spectrometry measurements were not used for these experiments. Cells were attached to the DEMS while placed inside a temperature chamber. Cells tested with the DEMS were prepared in the same manner described above, but not purged with any gas prior to connection to the DEMS. A pressure gauge (PX409-030AUSBH; Omega Engineering, Inc.; USA) outside the temperature chamber was used to track the pressure of the cell throughout the test, and the temperatures of both the gauge and cell were tracked throughout the test. The volume of the cell was measured by expanding the gas in the cell into an evacuated tube of known volume, while the cell was at room temperature. While full of argon gas, the cell was heated to 60 °C and allowed to rest for approximately 24 h to allow the pressure to stabilize. Once stabilized, the cell was purged with oxygen, and electrochemical tests were performed as described above. The ideal gas law was used to calculate the total moles of gas within the cell, and the rate of gas consumption and/or production was calculated by averaging the total moles of gas over 60 s intervals and using a Savitzky−Golay filter with polynomial order 2, filter width 31, and coefficients for the first derivative.[40]

Nuclear magnetic resonance (NMR) characterization was performed by dissolving a fragment of the collected PEO electrolyte in 0.7 mL of deuterated chloroform (D, 99.8%). The contents of the vial were rested overnight to allow the PEO electrolyte to dissolve. After resting, the fragment of undissolved Celgard was removed, and the solution was transferred to a NMR tube for ^{1}H NMR analysis. A Bruker AVANCE and Bruker AVANCE III-400 MHz NMR spectrometer was used.

Simulated ^{1}H NMR data were calculated using the ChemNMR package provided with ChemBioDraw Ultra (CambridgeSoft, PerkinElmer, USA), with a model solvent of $CDCl_3$ and 400 MHz.

Quantification of NMR was performed by integrating peaks in the following regions: 9.67−9.72 ppm (identified as aldehyde), 8.04−8.15 ppm (formate), 5.35−5.40 ppm (PEO-hydroperoxide/alcohol), 3.96−4.52 ppm (mixed oxidation products), and 3.42−3.90 ppm (ethylene oxide repeat unit). These areas were then converted into a relative number of each functional group, based on the number of protons predicted in that region for each functional group. Since both the aldehyde and formate groups are expected to produce peaks in the mixed oxidation products region (from the β-carbon protons), the expected area of these protons was subtracted from the measured area in that region, with the remaining area identified as ester functional groups.

RESULTS AND DISCUSSION

In order to establish the behavior of the PEO electrolyte in the Li−O_2 environment, two VC-free cells (Figure 1) were allowed to rest for 100 h at 60 °C in oxygen and argon. It was observed that the open-circuit voltage (OCV) of the oxygen cell rose from 2.9 V_{Li} to more than 3.5 V_{Li} after resting, while the OCV of the cell in argon rose only slightly, from 2.8 to 2.9 V_{Li} (Figure 2a).

For the oxygen cell, the OCV of the VC-free cell with BHT-free electrolyte rose throughout the duration of the test, starting around 2.95 V_{Li} and rising to 3.53 V_{Li} after 100 h. In contrast, the OCV of the argon cell reached a plateau after 5 h and remained steady throughout the test. In oxygen, visible electrolyte degradation was observed in addition to the rise in OCV. Portions of the electrolyte were liquid at room temperature after resting at OCV for 100 h in oxygen, and Celgard was required to prevent the cell from shorting. On the other hand, no significant changes in the electrolyte were observed for the cell in argon (Figure 2a, inset). The observed liquefaction indicates that chain scission of PEO occurred upon oxidation to break down the long backbone of PEO in oxygen at room temperature, which is discussed in detail using NMR data below. ^{1}H NMR data collected from a fragment of the rested electrolyte samples support the breakdown of the PEO

DOI: 10.1021/jp511794g
J. Phys. Chem. C 2015, 119, 6947−6955

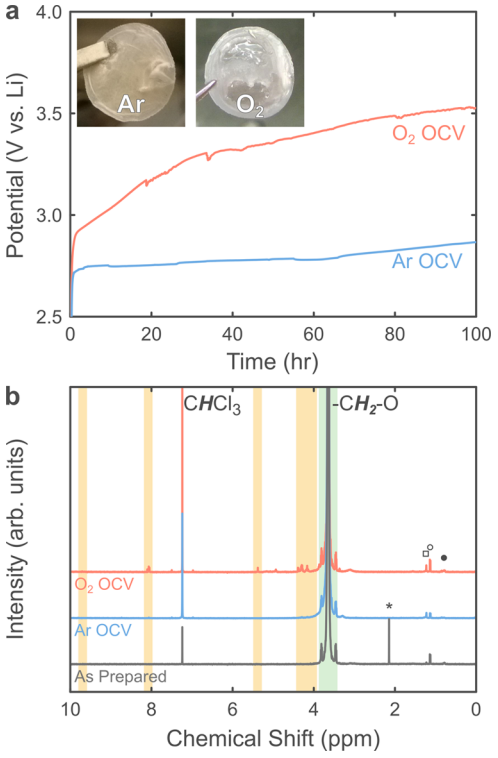

Figure 2. (a) OCV versus time of cells rested in oxygen and argon for 100 h. Inset shows optical images of the electrolyte samples after the rest. (b) NMR spectra of the rested electrolytes shown in (a). Peaks for PEO and chloroform (from the NMR solvent) are labeled, and peaks from the Celgard separator are identified by an open square (□) for polyethylene and open and closed circles (○ and ●) for polypropylene. Acetone contamination (from the NMR tube) is identified by an asterisk. Additional peaks attributed to the oxidation of PEO are highlighted in gold. Each plot was normalized to the area of the primary PEO peak highlighted in green.

electrolyte in oxygen but not in argon (Figure 2b). The as-prepared electrolyte shows peaks consistent with PEO, with additional peaks identified as trace amounts of Celgard, acetone, and chloroform. The sharp peak at 2.15 ppm is attributed to acetone contamination introduced while preparing the NMR samples. After exposure to oxygen, peaks were observed at shifts between 4.10−4.50 ppm, 5.35−5.40 ppm, 8.10−8.15 ppm, and 9.75 ppm.[41] In contrast, the electrolyte rested in argon shows no peaks in these regions. Although PEO is known to be susceptible to attack from atmospheric oxygen,[41−44] and the mechanism of this reaction is well understood,[42,43] we note that most PEO thermal oxidation experiments have shown this reaction to be slow, requiring experiments as long as 1000 h to show significant oxidation,[41,44] which is in contrast to the significant amount of oxidation observed in these experiments after only 100 h.

Similar resting experiments were performed on PEO with the antioxidant BHT in order to suppress the oxidation of PEO in the Li−O_2 cell (Figure S1, Supporting Information). The presence of BHT delayed the onset of the rise in OCV, but after 40 h the OCV was found to increase in oxygen. NMR analysis confirmed the presence of comparable oxidation products observed in the BHT-free electrolytes (Figure S1b, Supporting Information). The presence of BHT in the electrolyte may explain the relatively good performance of PEO-based Li−O_2 batteries shown in the very recent work by Balaish et al.[37] We note that the authors of that work do not report removing the BHT that is added to commercial PEO and further note that the limited capacity cycling shown in that work is estimated to have lasted less than 40 h. The BHT present in the electrolyte was likely irreversibly oxidized throughout the electrochemical tests presented in that work and therefore acted to suppress the total amount of electrolyte oxidation observed.

We further examined the effect of potentials greater than OCV on the oxidation kinetics of PEO electrolytes. Li−O_2 cells reported in the literature[11,14,17] are frequently charged at potentials of 3.6−4.0 V_{Li} or greater, and it is desirable to determine the effect of these higher potentials on the oxidation of the PEO electrolyte. We prepared several VC-free cells and held them potentiostatically at 3.6, 3.8, and 4.0 V_{Li} for 100 h in oxygen, along with a cell held at 3.8 V_{Li} in argon. The steady-state current (Figure S2, Supporting Information) observed for each of these cells was low (<350 nA) and was similar for cells tested in oxygen or argon, indicating that oxygen does not directly promote a measurable electrochemical reaction. NMR analysis of each electrolyte after oxidation at these potentials (Figure 3) shows the appearance of comparable peaks with

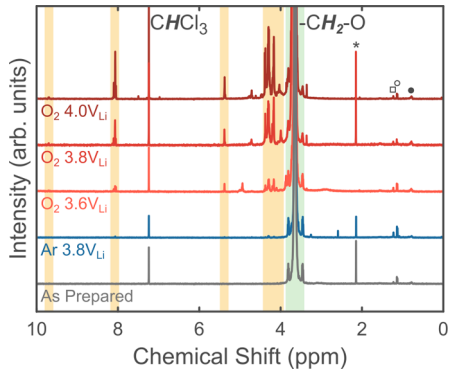

Figure 3. NMR spectra of PEO electrolytes after being charged potentiostatically for 100 h in oxygen at 3.6, 3.8, and 4.0 V_{Li}. Peaks are identified as described for Figure 2, and each plot is normalized to the area of the primary PEO peak (in green). The scale of this figure matches that of Figure 2b.

greater intensities in comparison to those identified from the OCV tests, which indicates that the amount of decomposition products upon oxidation increases with increasing potential. Similar to OCV in argon, applying potentials greater than OCV in argon produced extremely small oxidation peaks at 8.1 and 4.3 ppm.

Pressure tracking experiments showed that a significant amount of oxygen was consumed during tests both at OCV and at 4.0 V_{Li} and that the rate of consumption varied throughout the test. A digital pressure transducer was used to track and record the pressure of VC-free cells (using BHT-free electrolyte) over the duration of tests at OCV and at 4.0 V_{Li}, which allowed for the rate of oxygen consumption to be tracked (Figure 4). Because of the limited range of the pressure gauge, this test was performed with an initial oxygen pressure of 1.87 bar. For both tests, the rate of oxygen consumption was observed to be low and steadily increased for several hours. For the test at OCV, the rate of oxygen consumption increased steadily for the first 60 h, before stabilizing at 0.21 nmol/s for the remainder of the test. At 4.0 V_{Li}, the rate of oxygen consumption increased more rapidly at the beginning of the

DOI: 10.1021/jp511794g
J. Phys. Chem. C 2015, 119, 6947−6955

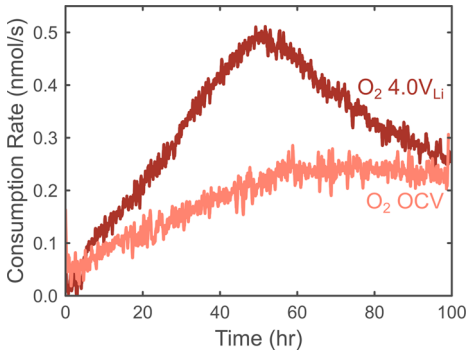

Figure 4. Oxygen consumption rate of VC-free cells (using BHT-free PEO electrolyte) rested at OCV and held at 4.0 V_{Li} as a function of time. Total moles of oxygen were calculated at each time point using pressure, temperature, and volume measurements in the ideal gas equation of state. The consumption rate was calculated as described in the experimental methods.

test, reaching a maximum of 0.50 nmol/s after 50 h, after which the rate of consumption gradually fell, approaching the same steady state consumption observed at OCV. The current passed was in agreement with the potentiostatic tests discussed above and stayed below 350 nA (3.6×10^{-3} nmol electron/s) throughout the test, more than 100 times smaller than the rate of oxygen consumption.

To further analyze the NMR results, we briefly discuss the mechanism of PEO thermal oxidation that has been reported in the literature previously.[41−44] The reaction mechanism that we propose here is similar to the mechanisms reported for the oxidation of liquid glymes when exposed to superoxide during discharge in Li−air systems[18,45,46] but does not rely on the presence of any superoxide radical species to initiate the reaction. Tsiouvaras et al. have also proposed a glyme decomposition mechanism in oxygen-free environments at very high voltages (≥4.9 V_{Li}),[47] a potential where PEO is already known to be unstable.[35] Similar to other auto-oxidation reactions of organic compounds, PEO is oxidized via radical chain reaction. A small number of peroxide species are formed via spontaneous reaction between PEO and molecular oxygen to form a PEO radical (−OC•HCH_2O−) and a hydroperoxide radical (Scheme 1, reaction I). This reaction is also known to occur much more quickly in the presence of singlet oxygen,[48,49] which has been proposed to form during discharge and charge of Li−air batteries.[36,46,50,51] The chain reaction is propagated when molecular oxygen reacts with the PEO radical to form a PEO-peroxy radical (reaction II), which then abstracts a hydrogen from another nearby ether group to form PEO-hydroperoxide and another PEO radical (reaction III). Chain branching (which further accelerates the reaction) occurs when PEO-hydroperoxide spontaneously decomposes to form a PEO-alkoxy radical and a hydroxyl radical (reaction IV). The hydroxyl radical can abstract a proton from a nearby PEO to form a PEO radical and water (reaction V) or react with PEO-hydroperoxide to form an ester or a PEO-peroxyl radical (reactions VIa,b). It has been reported that PEO-alkoxy radicals rapidly undergo β-scission to create a formate-terminated chain (reaction VII), rather than disproportionation to create an ester.[42] Chain termination occurs when two radicals recombine or disproportionate to form nonradical species. The large number of radical species present make listing all the possible reactions infeasible, but it has been shown that esters and

Scheme 1. PEO Auto-Oxidation Reaction Pathway[a]

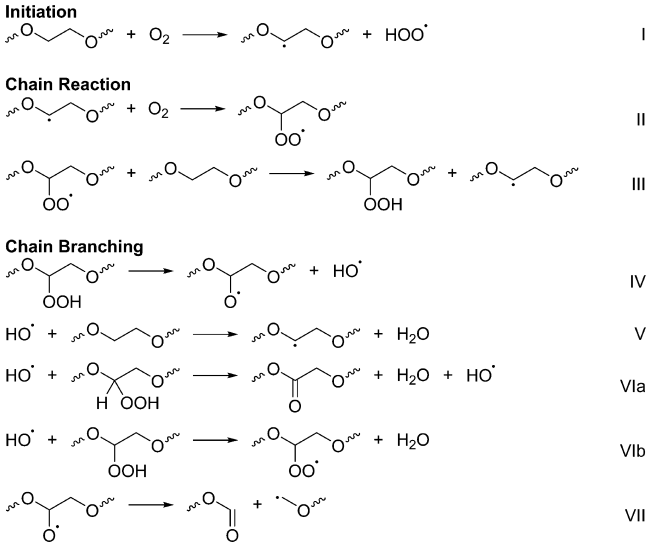

[a]Wavy bonds indicate the continuing PEO backbone. Termination reactions not shown.

formates are the dominant stable products of such PEO oxidation reactions.[42]

Little has been reported on the effect of elevated applied potentials on the auto-oxidation of PEO, such as those that occur during the charging of Li−O_2 batteries. We observed that the addition of oxygen to VC-free cells did not result in an increase in current, which remained very low with or without the presence of oxygen, indicating that the increased oxidation is not due to the bulk electro-oxidation of the PEO electrolyte but instead results from the acceleration of one or more of the reaction steps outlined above. Therefore, a quantitative analysis of the amount and relative ratios of the different products may allow further elucidation of the impact of elevated potential on PEO oxidation kinetics.

In the ^{1}H NMR spectra shown in Figures 2b and 3, the following peaks were associated with PEO oxidation: (i) 9.72 ppm (singlet), (ii) 8.10 ppm (group of singlets), (iii) 5.38 ppm (singlet, broadened), (iv) 4.1−4.5 ppm (group of many peaks). Peak i was identified as the proton bonded to the α-carbon of an aldehyde-terminated PEO chain (O═C*H*CH_2OCH_2−, calculated shift of 9.72 ppm). Peak ii was attributed to the α-carbon proton of a formate-terminated PEO chain (O═C*H*OCH_2CH_2−, calculated shift of 8.10 ppm). Peak iii was attributed to the α-carbon proton of PEO-hydroperoxide and/or a secondary alcohol (−OC*H*$OHCH_2O$− or −OC*H*$OOHCH_2O$−, calculated shift of 5.60 ppm). Group iv was attributed to the β-carbon protons for both aldehyde-terminated (O═CHCH_2*H*$_2OCH_2CH_2$−, calculated shift of 4.48 ppm) and formate-terminated PEO chains (O═CHOCH_2CH_2−, calculated shift of 4.28 ppm) and to in-chain esters (−OCH_2CH_2*H*$_2OC$═OCH_2O−, calculated shifts of 4.20 and 4.33 ppm). Note that other reports of PEO oxidation frequently report that no aldehydes are observed after oxidation and that the formation of formates is preferred over that of aldehydes when the alkoxy radical decomposes. The observation of aldehydes after oxidation in this work is consistent with these reports, as much more formate is observed than aldehyde, and the aldehyde products are only observed in the most highly oxidized samples.

DOI: 10.1021/jp511794g
J. Phys. Chem. C 2015, 119, 6947−6955

Integrated peak intensity was used to quantify the amount of each decomposition product. The number of each functional group relative to the number of ethylene oxide (EO) units for each of the samples shown in Figures 2 and 3 is plotted in Figure 5a. An overall extent of reaction was calculated (Figure 5b), comparing the number of aldehyde, formate, peroxide/alcohol, and ester reaction products with the total number of functional groups (including the large number of ethylene oxide groups). No oxidation peaks were observed in the as prepared sample, so it is excluded from Figure 5.

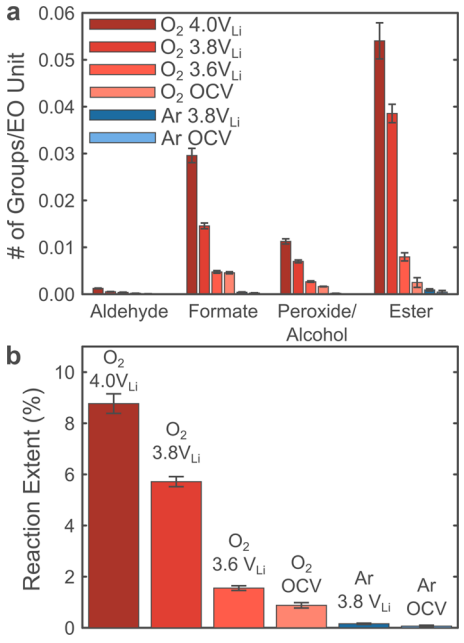

Figure 5. Quantification of oxidation products and total extent of oxidation. (a) Relative number of each type of functional group, shown for each of the experimental conditions. The as-prepared electrolyte exhibited no measurable peaks and is not shown. (b) Extent of oxidation and derived reaction rate for each of the experimental conditions. Each data point represents a cell that was held at the stated conditions for 100 h. Error bars represent the 95% confidence interval of estimated error due to integration.

Figure 5 clearly shows that more PEO is oxidized when exposed to potentials greater than OCV in oxygen. In contrast, samples treated in argon (with or without applied potential) are only slightly oxidized, with peaks barely rising above the background for all of the identified oxidation products. However, more careful examination of the relative amount of each oxidation product shows that applying a potential produces a different mixture of oxidation products. In particular, the potentiostatic samples have a much higher fraction of ester products, which make up 56 ± 5%, 64 ± 4%, and 50 ± 6% of all oxidation products for 4.0, 3.8, and 3.6 V_{Li}, respectively, while only 28 ± 12% of oxidation products are esters in the oxygen OCV sample. The opposite trend is observed for formates, which make up 31 ± 2%, 24 ± 1%, and 30 ± 2% of all oxidation products for 4.0, 3.8, and 3.6 V_{Li} respectively, but make up 52 ± 7% of oxidation products in the oxygen OCV sample (all uncertainties represent the 95% confidence interval).

Given the very low oxidative current relative to total oxygen consumption (as shown in Figure 4), we conclude that the increased potential causes more reaction chains to be created. This can be due to either an increased rate of initiation (reaction I) or an increased rate of chain branching (reaction IV). The primary chain reactions (reactions II and III) cannot be directly accelerated, as this would be expected to produce a measurable current on the same order as the rate of oxygen consumption. To postulate whether reaction I or IV is catalyzed, we consider the expected impact of increasing their reaction rates. If reaction I were to increase in rate with increasing voltage, larger numbers of PEO radicals would be produced, steadily increasing the number of PEO chains but not driving the reaction to favor any of the products. If reaction IV is catalyzed instead, causing PEO-hydroperoxide to break down more quickly and increasing the chain branching ratio, a larger number of PEO-alkoxy radicals would be produced. These alkoxy radicals would be expected to increase the fraction of formates in the oxidation products. In contrast, we observed that the fraction of formates in the overall oxidation products decreases with increasing potential; an increase in the number of esters was observed instead, which is consistent with more radicals undergoing more terminating reactions toward the end of oxidation. We conclude that the application of an oxidizing potential to a PEO electrolyte exposed to oxygen results in an increase in the rate of spontaneous PEO radical formation, which results in an increase in the total rate of PEO oxidation.

To show the direct impact the oxidation of PEO electrolytes has on the operation of Li−O_2 cells, we present the results of a PEO-based Li−O_2 cell using a VC cathode. Two cells are considered here: one which was singly discharged and another cycled five times (Figure 6). Both cells were discharged at 100 mAh/g_{VC}, and the cell that was cycled was subsequently charged to 4.2 V_{Li}. Both cells were started at the same time, and the cell that was singly discharged was held at 60 °C in oxygen until the cycling test completed. It is noted that the first-discharge capacity of a PEO-based Li−O_2 cell with a VC positive electrode (~1100 mAh/g_{VC}) is less than the capacity of similar cells using DME as an electrolyte reported elsewhere (~2800 mAh/g_{VC}).[52] The reduction may result from the high viscosity of the PEO electrolyte, which may inhibit the formation of large Li_2O_2 particles observed in Li−O_2 cells made with liquid electrolytes,[8,17,51−56] which is consistent with work suggesting that dissolution and diffusion of Li−O_2 discharge products are required to form large Li_2O_2 particles.[55−57] Excluding the reduced capacity, the profile of the first discharge for the PEO-based Li−O_2 cell is familiar:

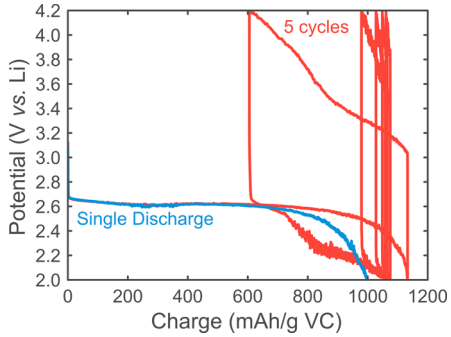

Figure 6. Performance of Li−O_2 cells using PEO-based electrolyte. Potential versus charge of a cell discharged once in oxygen and a cell cycled five times in oxygen. Charge is normalized to the mass of Vulcan carbon in the positive electrode.

DOI: 10.1021/jp511794g
J. Phys. Chem. C 2015, 119, 6947−6955

after a brief onset, a large plateau is observed near 2.5 V_{Li}, after which the voltage rapidly falls to 2.0 V_{Li}.

During the first charge, the profile initially appears to be similar to that of previously reported Li−O_2 charging processes in liquid electrolytes;[4,8,10,13,17,50] the potential quickly rises above 3.1 V_{Li} before rising more slowly to ∼3.6 V_{Li}. After this point, the voltage rises more rapidly, reaching the cutoff voltage of 4.2 V_{Li} (above which even liquid ether electrolytes are known to decompose).[11,58] Subsequent cycles show much poorer performance, with each subsequent cycle having lower capacity, a more sloped discharge profile, and an increasingly rapid rise in charging potential. The complete loss of cell performance after only five cycles shows that PEO degradation is significant even within the potential range that is ordinarily achievable for Li−O_2 batteries in the literature.[4,17]

An additional experiment was performed that tracked the consumption and production of gas throughout one discharge−charge cycle (Figure 7), using the same conditions listed above.

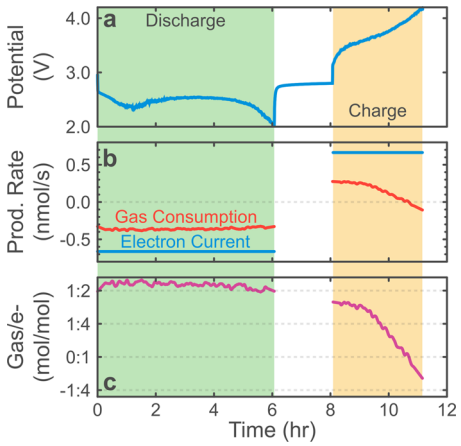

Figure 7. (a) Cell voltage vs time for a Li−O_2 cell cycled in O_2 with a VC cathode. (b) Gas production rate (red) and electron current (blue, converted to nmol/s of electrons) of the same cell. Negative production indicates consumption, and negative current indicates discharge. (c) Ratio of gas consumption rate to electron current plotted in (b). This ratio stayed close to 2 electrons/O_2 throughout discharge but deviated significantly from that value throughout charge. The negative gas to electron ratio indicates that gas is being consumed during charging.

The rate of gas consumption was near 2 electrons/O_2 throughout discharge (within the limit of the measurement accuracy), which is consistent with reported gas consumption rates in liquid glyme electrolytes.[11] However, the gas production during charge was far less than the ideal 2 electrons/O_2 expected for reversible oxidation of Li_2O_2. The performance was worse than has been reported for glyme electrolytes as well, which have been reported to have a gas production ratio of ∼2.6 electrons/O_2 for LiTFSI in DME;[11,47] the rate of gas production decayed throughout charge and even became negative as PEO auto-oxidation dominated over the expected production of O_2 due to Li_2O_2 oxidation.

Although mitigations may be available to extend the lifetime of a PEO-based Li−O_2 cell (such as reducing the oxygen partial pressure or removing all oxygen before charging), we assert that these techniques are neither sufficient nor feasible to protect the PEO for use as a practical device in commercial applications. We therefore suggest that further investigations into solid electrolyte-based Li−O_2 batteries focus on either eliminating PEO from the positive electrode (such as using ceramic electrolytes in the oxygen electrode)[27] or developing a compound that permanently inhibits the oxidation of PEO without interfering with the desired electrochemical reactions.

CONCLUSIONS

Development of a stable, solid-state Li−O_2 electrolyte remains a promising goal, as a carefully engineered solid electrolyte can allow for high oxygen transport, eliminate concerns about electrolyte evaporation, and protect the anode from oxygen, water, and other contaminants from the environment. We show here that PEO, widely studied as a solid lithium-conducting electrolyte, is not stable in the fully oxygenated environment of a Li−O_2 cell. Further work on the use of PEO and PEO-derived polymers as electrolytes for Li−O_2 and Li−air cells should focus on developing compounds that permanently inhibit the oxidation of PEO (without interfering in the electrochemical process), on developing protective layers that prevent the exposure of PEO to the oxygen environment, or on using materials not based on PEO for lithium conduction. Furthermore, the results presented here are an indication that other ether-based electrolytes (such as DME,[10,17,18,52] tetraethylene glycol dimethyl ether,[50,51,59−61] or trimethylsilyl oligo(ethylene oxide)[62]) may also be susceptible to oxidation directly from the environment,[63] in addition to the decomposition mechanisms that have already been explored for these compounds in Li−O_2 cells, and will likely be impacted by it when cycled many hundreds of times, as is commonly expected of commercially viable batteries. We conclude that the results presented here motivate further investigation into developing new oxidation-resistant electrolytes for Li−air batteries.

ASSOCIATED CONTENT

Supporting Information

Open-circuit rest in oxygen with BHT, current passed during potentiostatic tests. This material is available free of charge via the Internet at http://pubs.acs.org.

AUTHOR INFORMATION

Corresponding Author

*E-mail: shaohorn@mit.edu (Y.S.-H.).

Notes

The authors declare no competing financial interest.

ACKNOWLEDGMENTS

The authors acknowledge SAIT for providing funding for this research as well as the facilities as the Koch Institute for Integrative Cancer Research at MIT. C.V.A. acknowledges the GEM Fellowship and support by the Department of Defense (DoD) through the National Defense Science & Engineering Graduate (NDSEG) Fellowship Program.

ABBREVIATIONS

Li−air, lithium−air; DME, 1,2-dimethoxyethane; PEO, poly(ethylene oxide); V_{Li}, volts vs lithium; BHT, butylated hydroxytoluene; LiTFSI, lithium bis(trifluoromethane)sulfonimide; FEP, fluorinated ethylene propylene; VC, Vulcan carbon; DEMS, differential electrochemical mass spectrometer; NMR, nuclear magnetic resonance; OCV, open-circuit voltage; EO, ethylene oxide.

DOI: 10.1021/jp511794g
J. Phys. Chem. C 2015, 119, 6947−6955

REFERENCES

(1) Bruce, P. G.; Freunberger, S. A.; Hardwick, L. J.; Tarascon, J.-M. Li-O_2 and Li-S Batteries with High Energy Storage. *Nat. Mater.* **2012**, *11*, 19−29.

(2) Scrosati, B.; Hassoun, J.; Sun, Y.-K. Lithium-Ion Batteries. A Look into the Future. *Energy Environ. Sci.* **2011**, *4*, 3287−3295.

(3) Girishkumar, G.; McCloskey, B.; Luntz, A.; Swanson, S.; Wilcke, W. Lithium−Air Battery: Promise and Challenges. *J. Phys. Chem. Lett.* **2010**, *1*, 2193−2203.

(4) Lu, Y.-C.; Gallant, B. M.; Kwabi, D. G.; Harding, J. R.; Mitchell, R. R.; Whittingham, M. S.; Shao-Horn, Y. Lithium-Oxygen Batteries: Bridging Mechanistic Understanding and Battery Performance. *Energy Environ. Sci.* **2013**, *6*, 750−768.

(5) Gallagher, K. G.; Goebel, S.; Greszler, T.; Mathias, M.; Oelerich, W.; Eroglu, D.; Srinivasan, V. Quantifying the Promise of Lithium-Air Batteries for Electric Vehicles. *Energy Environ. Sci.* **2014**, *7*, 1555−1563.

(6) Gallant, B. M.; Lu, Y.-C.; Mitchell, R. R.; Kwabi, D. G.; Carney, T. J.; Thompson, C. V.; Shao-Horn, Y. In *The Lithium Air Battery*; Imanishi, N., Luntz, A. C., Bruce, P., Eds.; Springer: New York, 2014; pp 121−158.

(7) Sharon, D.; Etacheri, V.; Garsuch, A.; Afri, M.; Frimer, A. A.; Aurbach, D. On the Challenge of Electrolyte Solutions for Li−Air Batteries: Monitoring Oxygen Reduction and Related Reactions in Polyether Solutions by Spectroscopy and EQCM. *J. Phys. Chem. Lett.* **2012**, *4*, 127−131.

(8) Black, R.; Oh, S. H.; Lee, J.-H.; Yim, T.; Adams, B.; Nazar, L. F. Screening for Superoxide Reactivity in Li-O_2 Batteries: Effect on Li_2O_2/LiOH Crystallization. *J. Am. Chem. Soc.* **2012**, *134*, 2902−2905.

(9) Kwabi, D. G.; Ortiz-Vitoriano, N.; Freunberger, S. A.; Chen, Y.; Imanishi, N.; Bruce, P. G.; Shao-Horn, Y. Materials Challenges in Rechargeable Lithium-Air Batteries. *MRS Bull.* **2014**, *39*, 443−452.

(10) McCloskey, B. D.; Bethune, D. S.; Shelby, R. M.; Girishkumar, G.; Luntz, A. C. Solvents' Critical Role in Nonaqueous Lithium−Oxygen Battery Electrochemistry. *J. Phys. Chem. Lett.* **2011**, *2*, 1161−1166.

(11) McCloskey, B. D.; Bethune, D. S.; Shelby, R. M.; Mori, T.; Scheffler, R.; Speidel, A.; Sherwood, M.; Luntz, A. C. Limitations in Rechargeability of Li-O_2 Batteries and Possible Origins. *J. Phys. Chem. Lett.* **2012**, 3043−3047.

(12) Bryantsev, V. S.; Uddin, J.; Giordani, V.; Walker, W.; Addison, D.; Chase, G. V. The Identification of Stable Solvents for Nonaqueous Rechargeable Li-Air Batteries. *J. Electrochem. Soc.* **2013**, *160*, A160−A171.

(13) Walker, W.; Giordani, V.; Uddin, J.; Bryantsev, V. S.; Chase, G. V.; Addison, D. A Rechargeable Li−O_2 Battery Using a Lithium Nitrate/N,N-Dimethylacetamide Electrolyte. *J. Am. Chem. Soc.* **2013**, *135*, 2076−2079.

(14) Peng, Z.; Freunberger, S. A.; Chen, Y.; Bruce, P. G. A Reversible and Higher-Rate Li-O_2 Battery. *Science* **2012**, *337*, 563−566.

(15) Bryantsev, V. S.; Giordani, V.; Walker, W.; Blanco, M.; Zecevic, S.; Sasaki, K.; Uddin, J.; Addison, D.; Chase, G. V. Predicting Solvent Stability in Aprotic Electrolyte Li-Air Batteries: Nucleophilic Substitution by the Superoxide Anion Radical ($O_2^{-\bullet}$). *J. Phys. Chem. A* **2011**, *115*, 12399−12409.

(16) Schwenke, K. U.; Meini, S.; Wu, X.; Gasteiger, H. A.; Piana, M. Stability of Superoxide Radicals in Glyme Solvents for Non-Aqueous Li-O_2 Battery Electrolytes. *Phys. Chem. Chem. Phys.* **2013**, *15*, 11830−11839.

(17) Gallant, B. M.; Mitchell, R. R.; Kwabi, D. G.; Zhou, J.; Zuin, L.; Thompson, C. V.; Shao-Horn, Y. Chemical and Morphological Changes of Li−O_2 Battery Electrodes upon Cycling. *J. Phys. Chem. C* **2012**, *116*, 20800−20805.

(18) Freunberger, S. A.; Chen, Y. H.; Drewett, N. E.; Hardwick, L. J.; Barde, F.; Bruce, P. G. The Lithium-Oxygen Battery with Ether-Based Electrolytes. *Angew. Chem., Int. Ed.* **2011**, *50*, 8609−8613.

(19) Chen, Y.; Freunberger, S. A.; Peng, Z.; Bardé, F.; Bruce, P. G. Li−O_2 Battery with a Dimethylformamide Electrolyte. *J. Am. Chem. Soc.* **2012**, *134*, 7952−7957.

(20) Sharon, D.; Afri, M.; Noked, M.; Garsuch, A.; Frimer, A. A.; Aurbach, D. Oxidation of Dimethyl Sulfoxide Solutions by Electrochemical Reduction of Oxygen. *J. Phys. Chem. Lett.* **2013**, *4*, 3115−3119.

(21) Kwabi, D. G.; Batcho, T. P.; Amanchukwu, C. V.; Ortiz-Vitoriano, N.; Hammond, P.; Thompson, C. V.; Shao-Horn, Y. Chemical Instability of Dimethyl Sulfoxide in Lithium−Air Batteries. *J. Phys. Chem. Lett.* **2014**, *5*, 2850−2856.

(22) Fergus, J. W. Ceramic and Polymeric Solid Electrolytes for Lithium-Ion Batteries. *J. Power Sources* **2010**, *195*, 4554−4569.

(23) Kumar, B.; Kumar, J.; Leese, R.; Fellner, J. P.; Rodrigues, S. J.; Abraham, K. M. A Solid-State, Rechargeable, Long Cycle Life Lithium−Air Battery. *J. Electrochem. Soc.* **2010**, *157*, A50−A54.

(24) Zhang, T.; Imanishi, N.; Shimonishi, Y.; Hirano, A.; Takeda, Y.; Yamamoto, O.; Sammes, N. A Novel High Energy Density Rechargeable Lithium/Air Battery. *Chem. Commun.* **2010**, *46*, 1661−1663.

(25) Zhang, T.; Zhou, H. A Reversible Long-Life Lithium−Air Battery in Ambient Air. *Nat. Commun.* **2013**, *4*, 1817.

(26) Li, L.; Zhao, X.; Fu, Y.; Manthiram, A. Polyprotic Acid Catholyte for High Capacity Dual-Electrolyte Li-Air Batteries. *Phys. Chem. Chem. Phys.* **2012**, *14*, 12737−12740.

(27) Kitaura, H.; Zhou, H. Electrochemical Performance of Solid-State Lithium−Air Batteries Using Carbon Nanotube Catalyst in the Air Electrode. *Adv. Energy Mater.* **2012**, *2*, 889−894.

(28) Mohamed, S. N.; Johari, N. A.; Ali, A. M. M.; Harun, M. K.; Yahya, M. Z. A. Electrochemical Studies on Epoxidised Natural Rubber-Based Gel Polymer Electrolytes for Lithium−Air Cells. *J. Power Sources* **2008**, *183*, 351−354.

(29) Abraham, K. M.; Jiang, Z. A Polymer Electrolyte-Based Rechargeable Lithium/Oxygen Battery. *J. Electrochem. Soc.* **1996**, *143*, 1−5.

(30) Amanchukwu, C. V.; Harding, J. R.; Shao-Horn, Y.; Hammond, P. T. Understanding the Chemical Stability of Polymers for Lithium−Air Batteries. *Chem. Mater.* **2015**, *27*, 550−561.

(31) Fenton, D. E.; Parker, J. M.; Wright, P. V. Complexes of Alkali Metal Ions with Poly(Ethylene Oxide). *Polymer* **1973**, *14*, 589.

(32) Croce, F.; Appetecchi, G. B.; Persi, L.; Scrosati, B. Nanocomposite Polymer Electrolytes for Lithium Batteries. *Nature* **1998**, *394*, 456−458.

(33) Kim, G. T.; Jeong, S. S.; Xue, M. Z.; Balducci, A.; Winter, M.; Passerini, S.; Alessandrini, F.; Appetecchi, G. B. Development of Ionic Liquid-Based Lithium Battery Prototypes. *J. Power Sources* **2012**, *199*, 239−246.

(34) Gurevitch, I.; Buonsanti, R.; Teran, A. A.; Gludovatz, B.; Ritchie, R. O.; Cabana, J.; Balsara, N. P. Nanocomposites of Titanium Dioxide and Polystyrene-Poly(ethylene oxide) Block Copolymer as Solid-State Electrolytes for Lithium Metal Batteries. *J. Electrochem. Soc.* **2013**, *160*, A1611−A1617.

(35) Appetecchi, G. B.; Kim, G. T.; Montanino, M.; Alessandrini, F.; Passerini, S. Room Temperature Lithium Polymer Batteries Based on Ionic Liquids. *J. Power Sources* **2011**, *196*, 6703−6709.

(36) Hassoun, J.; Croce, F.; Armand, M.; Scrosati, B. Investigation of the O_2 Electrochemistry in a Polymer Electrolyte Solid-State Cell. *Angew. Chem., Int. Ed.* **2011**, *50*, 2999−3002.

(37) Balaish, M.; Peled, E.; Golodnitsky, D.; Ein-Eli, Y. Liquid-Free Lithium-Oxygen Batteries. *Angew. Chem., Int. Ed.* **2015**, *54*, 436−440.

(38) Oesten, R.; Heider, U.; Schmidt, M. Advanced Electrolytes. *Solid State Ionics* **2002**, *148*, 391−397.

(39) Lu, Y.-C.; Gasteiger, H. A.; Parent, M. C.; Chiloyan, V.; Shao-Horn, Y. The Influence of Catalysts on Discharge and Charge Voltages of Rechargeable Li−Oxygen Batteries. *Electrochem. Solid-State Lett.* **2010**, *13*, A69−A72.

(40) Savitzky, A.; Golay, M. J. E. Smoothing and Differentiation of Data by Simplified Least Squares Procedures. *Anal. Chem.* **1964**, *36*, 1627−1639.

(41) Han, S.; Kim, C.; Kwon, D. Thermal Degradation of Poly(ethyleneglycol). *Polym. Degrad. Stab.* **1995**, *47*, 203−208.

DOI: 10.1021/jp511794g
J. Phys. Chem. C 2015, 119, 6947−6955

(42) de Sainte Claire, P. Degradation of PEO in the Solid State: A Theoretical Kinetic Model. *Macromolecules* **2009**, *42*, 3469−3482.
(43) Dulog, V. L.; Storck, G. Die Oxydation von Polyepoxiden mit Molekularem Sauerstoff. *Makromol. Chem.* **1966**, *91*, 50−73.
(44) Yang, L.; Heatley, F.; Blease, T. G.; Thompson, R. I. G. A Study of the Mechanism of the Oxidative Thermal Degradation of Poly(ethylene oxide) and Poly(propylene oxide) Using 1H- and 13C-NMR. *Eur. Polym. J.* **1996**, *32*, 535−547.
(45) Bryantsev, V. S.; Faglioni, F. Predicting Autoxidation Stability of Ether- and Amide-Based Electrolyte Solvents for Li−Air Batteries. *J. Phys. Chem. A* **2012**, *116*, 7128−7138.
(46) Adams, B. D.; Black, R.; Williams, Z.; Fernandes, R.; Cuisinier, M.; Berg, E. J.; Novak, P.; Murphy, G. K.; Nazar, L. F. Towards a Stable Organic Electrolyte for the Lithium Oxygen Battery. *Adv. Energy Mater.* **2015**, *5*, 1400867.
(47) Tsiouvaras, N.; Meini, S.; Buchberger, I.; Gasteiger, H. A. A Novel On-Line Mass Spectrometer Design for the Study of Multiple Charging Cycles of a Li-O_2 Battery. *J. Electrochem. Soc.* **2013**, *160*, A471−A477.
(48) Hu, J.; Xu, K.; Jia, Y.; Lv, Y.; Li, Y.; Hou, X. Oxidation of Ethyl Ether on Borate Glass: Chemiluminescence, Mechanism, and Development of a Sensitive Gas Sensor. *Anal. Chem.* **2008**, *80*, 7964−7969.
(49) Kaplan, M. L.; Kelleher, P. G. On the Mechanism of Polyethylene Photodegradation: The Oxidation of Terminal Olefins and Saturated Centers with Singlet Oxygen. *J. Polym. Sci., Part B: Polym. Lett.* **1971**, *9*, 565−568.
(50) Lu, Y.-C.; Shao-Horn, Y. Probing the Reaction Kinetics of the Charge Reactions of Nonaqueous Li−O_2 Batteries. *J. Phys. Chem. Lett.* **2012**, *4*, 93−99.
(51) Black, R.; Lee, J.-H.; Adams, B.; Mims, C. A.; Nazar, L. F. The Role of Catalysts and Peroxide Oxidation in Lithium−Oxygen Batteries. *Angew. Chem., Int. Ed.* **2013**, *52*, 392−396.
(52) Lu, Y. C.; Kwabi, D. G.; Yao, K. P. C.; Harding, J. R.; Zhou, J. G.; Zuin, L.; Shao-Horn, Y. The Discharge Rate Capability of Rechargeable Li-O_2 Batteries. *Energy Environ. Sci.* **2011**, *4*, 2999−3007.
(53) Mitchell, R. R.; Gallant, B. M.; Thompson, C. V.; Shao-Horn, Y. All-Carbon-Nanofiber Electrodes for High-Energy Rechargeable Li-O_2 Batteries. *Energy Environ. Sci.* **2011**, *4*, 2952−2958.
(54) Mitchell, R. R.; Gallant, B. M.; Shao-Horn, Y.; Thompson, C. V. Mechanisms of Morphological Evolution of Li_2O_2 Particles during Electrochemical Growth. *J. Phys. Chem. Lett.* **2013**, *4*, 1060−1064.
(55) Schwenke, K. U.; Metzger, M.; Restle, T.; Piana, M.; Gasteiger, H. A. The Influence of Water and Protons on Li_2O_2 Crystal Growth in Aprotic Li-O_2 Cells. *J. Electrochem. Soc.* **2015**, *162*, A573−A584.
(56) Aetukuri, N. B.; McCloskey, B. D.; García, J. M.; Krupp, L. E.; Viswanathan, V.; Luntz, A. C. Solvating Additives Drive Solution-Mediated Electrochemistry and Enhance Toroid Growth in Non-Aqueous Li−O_2 Batteries. *Nat. Chem.* **2015**, *7*, 50−56.
(57) Meini, S.; Piana, M.; Tsiouvaras, N.; Garsuch, A.; Gasteiger, H. A. The Effect of Water on the Discharge Capacity of a Non-Catalyzed Carbon Cathode for Li-O_2 Batteries. *Electrochem. Solid-State Lett.* **2012**, *15*, A45−A48.
(58) Ottakam Thotiyl, M. M.; Freunberger, S. A.; Peng, Z.; Bruce, P. G. The Carbon Electrode in Nonaqueous Li−O_2 Cells. *J. Am. Chem. Soc.* **2012**, *135*, 494−500.
(59) Meini, S.; Piana, M.; Beyer, H.; Schwämmlein, J.; Gasteiger, H. A. Effect of Carbon Surface Area on First Discharge Capacity of Li-O_2 Cathodes and Cycle-Life Behavior in Ether-Based Electrolytes. *J. Electrochem. Soc.* **2012**, *159*, A2135−A2142.
(60) Laoire, C.; Mukerjee, S.; Plichta, E. J.; Hendrickson, M. A.; Abraham, K. M. Rechargeable Lithium/TEGDME- $LiPF_6$/O_2 Battery. *J. Electrochem. Soc.* **2011**, *158*, A302−A308.
(61) Jung, H.-G.; Hassoun, J.; Park, J.-B.; Sun, Y.-K.; Scrosati, B. An Improved High-Performance Lithium−Air Battery. *Nat. Chem.* **2012**, *4*, 579−585.
(62) Zhang, Z.; Lu, J.; Assary, R. S.; Du, P.; Wang, H.-H.; Sun, Y.-K.; Qin, Y.; Lau, K. C.; Greeley, J.; Redfern, P. C.; et al. Increased Stability Toward Oxygen Reduction Products for Lithium-Air Batteries with Oligoether-Functionalized Silane Electrolytes. *J. Phys. Chem. C* **2011**, *115*, 25535−25542.
(63) Glastrup, J. Degradation of Polyethylene Glycol. A Study of the Reaction Mechanism in a Model Molecule: Tetraethylene Glycol. *Polym. Degrad. Stab.* **1996**, *52*, 217−222.

DOI: 10.1021/jp511794g
J. Phys. Chem. C 2015, 119, 6947−6955